IEEE Access
Multidisciplinary | Rapid Review | Open Access Journal

Received May 27, 2019, accepted June 7, 2019, date of publication June 12, 2019, date of current version July 1, 2019.

Digital Object Identifier 10.1109/ACCESS.2019.2922408

Investigation of Total-Ionizing Dose Effects on the Two-Dimensional Transition Metal Dichalcogenide Field-Effect Transistors

SHUYUN ZHENG, YUN ZENG, AND ZHUOJUN CHEN, (Member, IEEE)
School of Physics and Electronics, Hunan University, Changsha 410082, China

Corresponding author: Zhuojun Chen (zjchen@hnu.edu.cn)

This work was supported in part by the National Natural Science Foundation of China under Grant 6180405, in part by the Natural Science Foundation of Hunan Province under Grant 2019JJ50092, in part by the Fundamental Research Funds for the Central Universities under Grant 2014YJS137, and in part by the Technology Program of Changsha under Grant kq1804001.

ABSTRACT Due to the excellent electrical properties, the emerging field-effect transistor (FET) based on two-dimensional transition metal dischalcogenide (TMD) is an excellent candidate for future space applications. However, the device performance is significantly impacted by total-ionizing dose (TID) effects. In this paper, the TID effects of TMD FETs are investigated comprehensively by means of developing a surface-potential based drain current model. Not only the radiation-induced trapped charges but also mobility degradation are incorporated into the proposed model. The model approach is demonstrated for a bottom-gated TMD FET, that simulation results are in good agreement with the experimental data. Based on the validity of the proposed method, the influence of TID effects on the TMD-on-insulator (TMDOI) FET is presented and discussed under different total dose levels. The results show that surface potential is strongly dependent on the oxide trapped charges, resulting in a major contribution to the negative shift of threshold voltage and the significant increase of leakage current. Besides, the interface trapped charges reduce the effective carrier mobility, which plays a dominant role on the decrease of transconductance and increase of subthreshold voltage swing. Finally, this paper gives insight into some possible mitigation techniques of TID effects on TMD FETs.

INDEX TERMS Transition metal dichalcogenide (TMD), field-effect transistor (FET), total ionizing dose (TID), surface potential, compact model.

I. INTRODUCTION

Recently, it is reported that two-dimensional (2D) semiconductors including transition metal dischalcogenides (TMDs) show great potential for extending Moore's law due to their excellent electrical properties, although some practical challenges need to be overcome [1]. MoS_2 is one of the most popular TMDs, which has a finite band gap of 1.8 eV and controllable atomic-scale thickness [2], [3]. Besides, it is suitable to act as channel material to form field-effect transistors (FETs) with intrinsically thin-body on insulator. Some MoS_2 based field-effect transistors (MoS_2 FETs) were successfully fabricated and proven to obtain high on/off current ratios and mobility [4], which could meet the requirement of low-power and high-speed integrated circuits for future space applications and other circumstance.

However, the TMD FETs may suffer from radiation effects that all the devices need to face in the complex space environment or other high-intensity radiation scenarios, such as nuclear power plants, or some anti-explosive radiation scenarios. Among them, total-ionizing dose (TID) effect and single-event effect (SEE) are commonly taken into consideration [5], [6]. The SEE is caused by radiation particles which can penetrate semiconductor material and deposit charge in the active regions, leading to instantaneous damages [7]. For TMD FETs, the impacts of SEEs should be negligible due to their extremely small sensitive volume. However, the TID effect which represents the long-term accumulation of ionizing dose is taking place on TMD based FETs, which may degrade the electrical performance or even result in functional failure. In previous studies, some radiation experiments have already been performed to investigate the TID response of TMD devices. Zhang et.al. and Kim et.al. observed that the drain current of MoS_2 transistors decreased significantly

The associate editor coordinating the review of this manuscript and approving it for publication was Anisul Haque.

2169-3536 © 2019 IEEE. Translations and content mining are permitted for academic research only.
Personal use is also permitted, but republication/redistribution requires IEEE permission.
See http://www.ieee.org/publications_standards/publications/rights/index.html for more information.

after 10-keV x-ray irradiation and proton irradiation, respectively [8], [9].

To further understand the basic mechanism contributing to ionizing radiation effects on field-effect transistors, some compact models have been developed. Zebrev et.al. proposed a compact drain current model for irradiated MOSFETs, compatible with BSIM model [10]. Esqueda et.al. developed a surface-potential-based modeling approach for bulk and SOI MOSFETs under TID exposure, which described the TID-induced charges from oxide trapped charges and interface traps [11]. Jazaeri et.al. presented a charge-based model to address the main mechanism of radiation-induced damages in double-gate MOSFETs [12]. However, the radiation damages in TMD FETs from the aspect of physics-based model are rarely considered. The compact model for TMD FETs have already been developed with consideration of extrinsic effects such as interface traps [13]. At present, the radiation physics-based model for TMD FETs is still lacking.

In this paper, a compact model is presented for bottom-gated TMD FET and TMD-on-insulator (TMDOI) FET with the consideration of the impact of ionizing radiation, where an N-type TMD like MoS_2 is used as the channel material. The rest of the paper is organized as follows. Section II focuses on the description of model approach, which includes the relationship between total dose ionizing (TID) and trapped charges, and the explicit expression of the mobility degradation. Section III provides the model formulation of the bottom-gated TMD FET and TMD-on-insulator (TMDOI) FET by solving Poisson's equation. Section IV verifies the proposed model and discusses the electrical performance shifts after irradiation for the bottom-gated TMD FET and TMDOI FET. Finally, conclusions are given in Section V.

II. MODELING APPROACH

A. ANALYTICAL INTRODUCTION OF N_{ot} AND N_{it}

When a TMD FET is exposed to ionizing radiation, excessive electron-hole pairs are generated and deposited in the oxide layer. Most of them will not recombine for the reason that the mobility of electrons is greater than that of holes. Under the localized electric field, the electrons will be swept to the electrode with higher potential, and the holes will move to the TMD/SiO_2 interface. Finally, the holes are captured in the oxide bulk or to the interface.

Fig. 1 shows the band diagram of a N-type TMD FET with positive gate voltage bias, and the ionization-induced defect densities can be described as oxide charged trap density (N_{ot}) and the semiconductor/oxide interface trap density (N_{it}), which are obtained as follows [14]

$$N_{ot} = N_t \left[\frac{1}{2} t_{ox} + \frac{e^{-\sigma pt^k gf_y t_{ox} D}}{-\sigma_{pt} k_g f_y t_{ox} D} + \frac{e^{-\sigma_{pt} k_g f_y t_{ox} D} - 1}{\left(-\sigma_{pt} k_g f_y t_{ox} D\right)^2 t_{ox}} \right] \quad (1)$$

$$N_{it} = N_{tmd-h} \left(1 - e^{-\sigma_{dh} \sigma_{it} N_{dh} k_g f_y t_{ox}^2 D/2} \right) \quad (2)$$

where D represents for the total dose. N_t, k_g and f_y are the hole trap concentration in the oxide layer, the number of electron-hole pairs per unit dose and the hole yield. σ_{pt}, N_{dh}, σ_{dh} and N_{tmd-h} are the hole capture, the trap concentration of hydrogen, the trapped cross section of holes and the dangling bond density of hydrogen passivation, respectively.

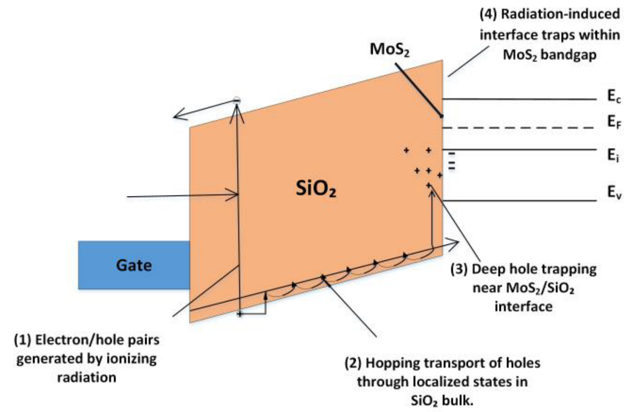

FIGURE 1. The band diagram of a TMD FET under positive gate voltage bias and the four basic steps of charge capture under total ionizing dose effects.

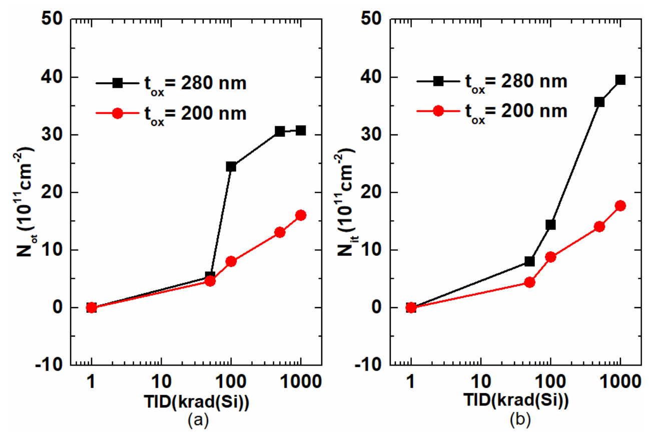

FIGURE 2. N_{ot} (a) and N_{it} (b) variations as a function of TID level changing from 0 krad(Si) to 1000 krad(Si), for the devices with different oxide thicknesses.

The value of N_{ot} and N_{it} as a function of TID level with different oxide thicknesses are plotted in Fig. 2 (a) and (b), respectively. From Fig. 2 (a), it can be observed that N_{ot} gradually grows with increasing TID level, and becomes saturation when total ionizing dose is greater than 500 krad(Si). And N_{it} significantly increases with total dose, as shown in Fig. 2 (b). Besides, it shows that both N_{ot} and N_{it} positively correlate with oxide thickness (t_{ox}). Nevertheless, the growth trend will slow down when oxide thickness (t_{ox}) is larger, which is supposed to be the limitation of the dangling bond density of hydrogen passivation in oxide layer, and this leads to the saturation of N_{it} and N_{ot}.

B. MOBILITY DEGRADATION CAUSED BY TID EFFECTS

Due to the additional carrier scattering caused by the total ionizing dose effects, the mobility degradation of a TMD FET should be taken into consideration. In previous studies,

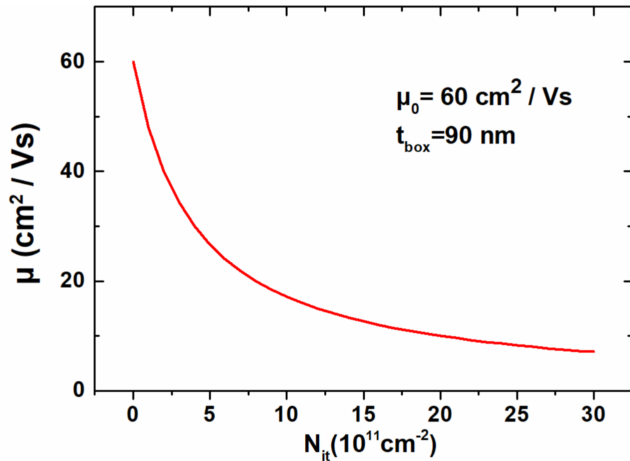

FIGURE 3. The effective mobility degradation as a function of interface trap density (N_{it}).

the effect of interface trapped charges is predominant, and the effect of oxide trapped charges can be ignored [15]. Therefore, the effective carrier mobility after radiation exposure can be expressed as:

$$\mu = \frac{\mu_0}{1 + \alpha_{it} N_{it}} \tag{3}$$

where μ_0 respectively represent the mobility before irradiation, and α_{it} is a fitting parameter. Fig. 3 plots the relationship between the irradiated carrier mobility versus oxide interface trap density. Assuming the initial mobility is 60 cm^2/Vs, the irradiated mobility decreases with interface trapped charges. After irradiation up to 1000 krad(Si), N_{it} increases to around 15×10^{11} cm^{-2} with oxide thickness of 90 nm, which corresponds to effective mobility degradation from 60 cm^2/Vs to 12.5 cm^2/Vs. It is because that carriers will scatter on the surface and go through the process of capturing and releasing, which directly reduces the mobility.

C. TOTAL CHARGE INDUCED BY TID EFFECTS

For simplicity, we assume that N_{ot} is constant for a certain total dose level, which will not respond to the variations of Fermi level (E_f). Nevertheless, the interface traps have short time constants and can be assumed to respond instantaneously by changing their state of occupancy, and thus interface trapped charge is determined by E_f, which is related to surface potential φ_s and can be expressed as

$$Q_{it} = -qD_{it}(\varphi_s - \phi_b), \tag{4}$$

where $D_{it} = N_{it}/\phi_b$ represents for the number of interface traps per unit area per unit energy, and ϕ_b is the potential difference between mid-gap and the Fermi level.

Therefore, the total charge resulting from TID effects can be written as follows:

$$Q_{tid} = Q_{ot} + Q_{it} = qN_{ot} - qD_{it}(\varphi_s - \phi_b). \tag{5}$$

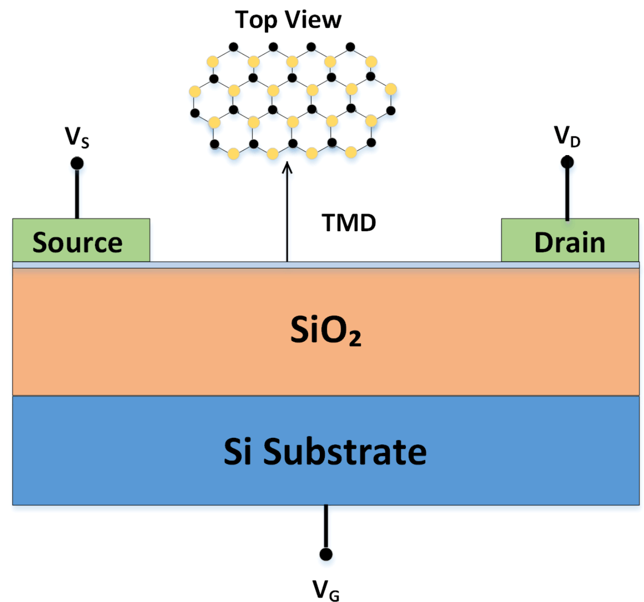

FIGURE 4. The cross-sectional diagram of a bottom–gated TMD FET.

It means that the contribution of fixed charge and interface trapped charge to Q_{tid} is mainly dependent by N_{ot} and D_{it}.

III. MODEL FORMULATION

A. DRAIN CURRENT MODEL FOR A BOTTOM–GATED TMD FET

For a monolayer TMD FET as shown in Fig. 4, the potential along the thickness can be assumed to constant due to its extremely thin body. By means of gradual channel approximation and Gauss's law, the relationship between the gate voltage (V_g) and the semiconductor charge density (Q_s) can be expressed as

$$Q_s = \varepsilon_{ox} E_{ox} + Q_t = C_{ox}(V_g - \phi_{ms} - \varphi_s) + Q_{tid} \tag{6}$$

where ϕ_{ms} is the work function difference between gate electrode and TMD layer, C_{ox} is the capacitance of the gate oxide.

Then, the combination of (1) and (4) yields:

$$Q_s = qN_{ot} - qD_{it}(\varphi_s - \phi_b) + C_{ox}(V_g - \phi_{ms} - \varphi_s). \tag{7}$$

After rearranging, (6) is unified as follows:

$$Q_s = C_{ox}(V_{geff} - \sigma\varphi_s) + Q_f \tag{8}$$

where $V_{geff} = V_g - \phi_{ms}$, $\sigma = 1 + qD_{it}/C_{ox}$, and $Q_f = q(N_{ot} + D_{it}\phi_b)$.

Besides, the total semiconductor charge density can be modeled in terms of density of state (DOS) and the Fermi statistics [$f(E - E_f)$] [16], [17]. For a TMD FET, the total charge density can also be expressed as

$$Q_s = -q \int_{E_c}^{\infty} N_{DOS}(E) f(E - E_f) dE \tag{9}$$

where E_c is the conduction band minima, and E_f is the Fermi energy.

After calculation, Q_s can be expressed as

$$Q_s = q^2 N_{DOS} v_{th} \ln\left(1 + e^{u/v_{th}}\right). \tag{10}$$

where $v_{th} = kT/q$ is the thermal voltage, $u = \varphi_s - V$, and V is the quasi-Fermi potential.

After simplification, (10) can be rewritten as follows

$$\frac{u}{v_{th}} = \ln\left(e^{\frac{Q_s}{q^2 v_{th} N_{DOS}}} - 1\right), \tag{11}$$

Similar with [18], by using the first order Taylor series expansion of $e^{\frac{Q_s}{q^2 v_{th} N_{DOS}}}$, it can be given as

$$\frac{u}{v_{th}} = \ln\left(\frac{Q_s}{q^2 v_{th} N_{DOS}}\right), \tag{12}$$

which is verified in Appendix.

Combining (8) and (12), we can obtain

$$\varphi_s - V = v_{th} \ln\left[\frac{C_{ox}(V_{geff} - \sigma\varphi_s) + Q_f}{q^2 N_{DOS} v_{th}}\right], \tag{13}$$

By using the Lambert-W function, φ_s can be expressed as

$$\varphi_s = \frac{V_{gg}}{\sigma} - v_{th} W\left[\frac{q^2 N_{DOS}}{\sigma C_{ox}} e^{\frac{V_{gg} - \sigma V}{\sigma v_{th}}}\right], \tag{14}$$

where $V_{gg} = V_{geff} + \frac{Q_f}{C_{ox}}$.

The surface potential at the source and drain sides can be defined as φ_{ss} and φ_{sd}, by substituting $V = 0$ and $V = V_{ds}$ into (8), respectively. Then we can obtain the total charge density at the source and drain sides as follows

$$Q_{ss} = C_{ox}(V_{geff} - \sigma\varphi_{ss}) + Q_f, \tag{15}$$
$$Q_{sd} = C_{ox}(V_{geff} - \sigma\varphi_{sd}) + Q_f. \tag{16}$$

According to the drift-diffusion transport model and the current continuity condition, the drain current of the TMD FET can be given as

$$I_{ds} = \mu W_g \int_s^d Q_s \frac{dV}{du}\frac{du}{dx}, \tag{17}$$

where W_g is the channel width, and μ is the mobility. Using (8), $\frac{dV}{du}$ can be expressed as

$$\frac{dV}{du} = -1 - \frac{1}{\sigma C_{ox}}\frac{dQ_s}{du}. \tag{18}$$

Substituting (18) into (17) and followed by integration, the drain current model can be written as

$$I_{ds} = \frac{\mu W_g}{L_g}\left[\frac{(Q_{ss}^2 - Q_{sd}^2)}{2\sigma C_{ox}} - q^2 v_{th} N_{DOS} \int_{u_s}^{u_d} \ln(1 + e^{u/v_{th}}) du\right], \tag{19}$$

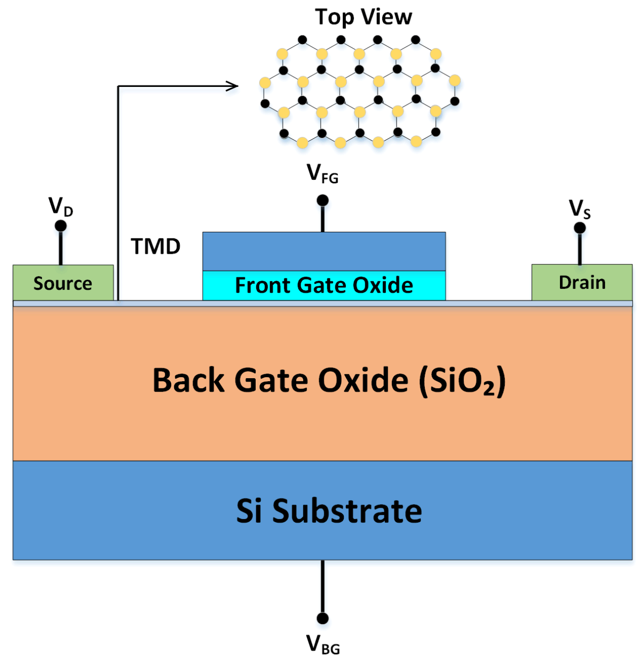

FIGURE 5. Cross-sectional diagram of TMDOI FET.

where L_g is the channel length, $u_s = \varphi_{ss}$, $u_d = \varphi_{sd} - V_{ds}$. From (12), (15) and (16), the drain current can be obtained as a function of u_s and u_d

$$\begin{aligned} I_{ds} &= \frac{\mu W_g}{L_g}\left[C_{ox}\left(V_{geff} + \frac{Q_f}{C_{ox}} - \sigma\frac{V_{ds} + u_d + u_s}{2}\right)(V_{ds} + u_d - u_s) \right. \\ &\quad \left. - q^2 v_{th} N_{DOS} \int_{u_s}^{u_d} \ln\left(1 + e^{u/v_{th}}\right) du\right] \\ &= I_{ds0} + \frac{\mu W_g \overline{Q_{tid}}}{L_g}(\varphi_{sd} - \varphi_{ss}) \end{aligned} \tag{20}$$

where

$$I_{ds0} = \frac{\mu W_g}{L_g}\left[\frac{Q_{ss}^2 - Q_{sd}^2}{C_{ox}} - q^2 v_{th} N_{DOS} \int_{u_s}^{u_d} \ln\left(1 + e^{u/v_{th}}\right) du\right], \tag{21}$$

$$\overline{Q_{tid}} = qN_{ot} - qD_{it}\left(\frac{\varphi_{sd} + \varphi_{ss}}{2} - \phi_b\right). \tag{22}$$

Without consideration of total-ionizing dose effects, the average total charge resulted from irradiation $\overline{Q_{tid}}$ equals to zero, and then the drain current expression can be obtained by (21), which is the same with the derivation reported in [19]. It is worth noticing that I_{ds0} is also influenced by the radiation exposure, for the reason that surface potential is a function of N_{ot} and D_{it} according to (14).

B. DRAIN CURRENT MODEL FOR A TMD-ON-INSULATOR (TMDOI) FET

The schematic of a TMDOI FET is shown in Fig. 5. For simplicity, only the impact of TID effect in back gate oxide

is taken into consideration for the reason that the back gate oxide is much thicker than the front gate oxide. According to the Poisson equation, the charge densities at the front and back gate can be expressed as

$$Q_{sf} = C_{oxf}(V_{fg} - \phi_{msf} - \varphi_s), \quad (23)$$
$$Q_{sb} = C_{oxb}(V_{bg} - \phi_{msb} + \phi_{ntb} - \varphi_s), \quad (24)$$

where C_{oxf} and C_{oxb} are the front and back gate oxide capacitances respectively, φ_s is the surface electrostatic potential, and ϕ_{ntb} can be given as

$$\phi_{ntb} = \frac{Q_{tid}}{C_{oxb}} = \frac{Q_f - qD_{it}\varphi_s}{C_{oxb}}. \quad (25)$$

Furthermore, the total charge density (Q_s) in the TMDOI FET can be written as follows

$$Q_s = Q_{sf} + Q_{sb} = C_{oxf}\left[V'_{geff} - (1+\lambda)\varphi_s + \lambda\phi_{ntb}\right] \quad (26)$$

where $V'_{geff} = V_{fg} + \lambda V_{bg} - V_{t0}$, $V_{t0} = \phi_{msf} + \lambda\phi_{msb}$, and $\lambda = C_{oxb}/C_{oxf}$.

After rearranging, the total charge density can be obtained as

$$Q_s = C_{oxf}(V'_{geff} - \sigma'\varphi_s) + Q_f \quad (27)$$

where $\sigma' = 1 + \lambda\left(1 + \frac{qD_{it}}{C_{oxb}}\right)$.

Applying the method mentioned in Part A, the surface potential for a TMDOI FET can be given as

$$\varphi_s = \frac{V'_{gg}}{\sigma'} - v_{th}W\left[\frac{q^2 N_{DOS}}{\sigma' C_{ox}} e^{\frac{V'_{gg} - \sigma' V}{\sigma' v_{th}}}\right] \quad (28)$$

where $V'_{gg} = V'_{geff} + Q_f/C_{ox}$. Similarly, the drain current for a TMDOI FET can be calculated using (20) by replacing V_{gg} and σ with V'_{gg} and σ', respectively. It is worth noticing that V'_{gg} is a function of N_{ot}, while σ' is a function of D_{it}.

IV. RESUITS AND DISSCUSSIONS

To verify the proposed surface-potential-based TID model, numerical simulations of a bottom-gated TMD FET are performed, compared with the experimental results extracted from [8]. Fig. 6 shows the transfer characteristic curves for a TMD FET ($W_g = 3\mu$m, $L_g = 2.3\mu$m, $t_{ox} = 280$nm), changing total dose from 0 to 1000 krad(Si). It can be observed that the simulation results obtained from (20) are in good agreement with the experimental results. In the following discussions, we mainly focus on the total ionizing dose effects of a TMDOI FET.

The surface potentials as a function of front gate voltage and back gate voltage are shown in Fig. 7. It indicates that TID has a great impact on surface potential, which increases from −0.54 V to −0.27 V at $V_{fg} = -0.5$ V, and $V_{bg} = 0$ V. Besides, the lower front or back gate voltage, the higher surface potential shift can be seen. It is mainly because that the channel is weakly controlled by the small external gate voltage, and on the contrary strongly dependent on the positive radiation-trapped charge. What's more, the positive shift of φ_s can be

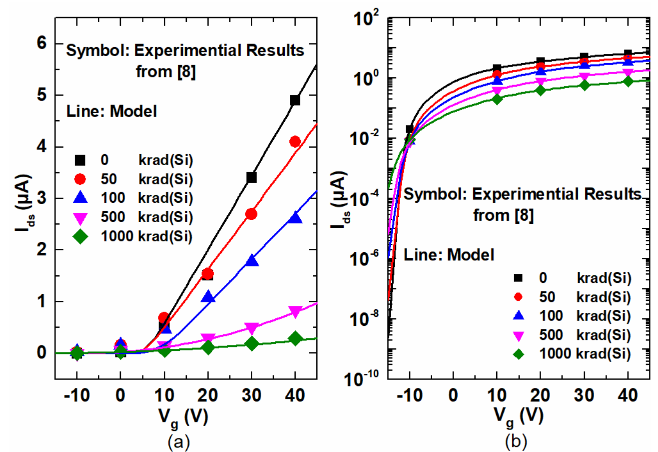

FIGURE 6. The transfer characteristics of a bottom-gated TMD FET (W_g =3μm, L_g =2.3μm, t_{ox} =280nm) under different TID levels. In the graph, symbol stands for the experimental results extracted from [8], and line stands for the numerical simulation results using (20).

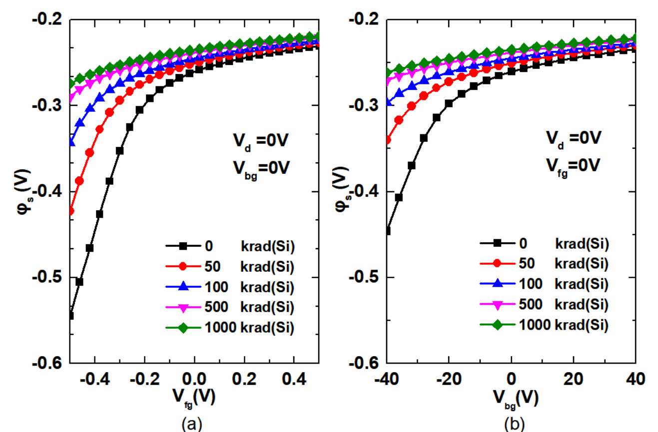

FIGURE 7. Numerical simulations of the surface potential at the source of a TMDOI device as a function of V_{fg} (a) and V_{bg} (b), for various total-ionizing dose levels (0krad(Si), 50krad(Si), 100krad(Si), 500krad(Si), 1000krad(Si)).

reduced by applying negative back gate voltage. According to (28), due to the thick back gate oxide, a relatively large negative voltage should be applied to the back gate so as to eliminate the TID-induced surface potential shift.

In order to distinguish the impact of oxide trapped charge and the interface trapped charge, the surface potential variations are shown in Fig. 8 (a). It can be found that for a certain TID exposure, the contribution of N_{ot} to the surface potential increase is dominant. Besides, the thickness of the back gate oxide affects the surface potential significantly, which is plotted in Fig. 8 (b). Thicker back gate oxide is considered to generate more oxide charge, which leads to the greater contribution of N_{ot}, and finally reflects in the variation of surface potential.

The drain currents of the TMDOI FET as a function of front gate voltage and back gate voltage are shown in Fig. 9 (a) and (b), respectively. With accumulating ionizing dose, the leakage current grows rapidly. It is because that at the same low front gate voltage, higher surface potential

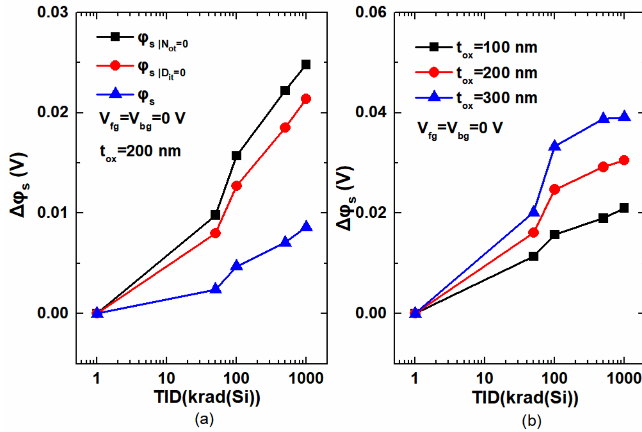

FIGURE 8. Surface potential variations for a TMDOI device ($V_{fg} = V_{bg} = V_d = 0$) versus TID level, compared to the situations without consideration of N_{ot} and D_{it}, respectively.

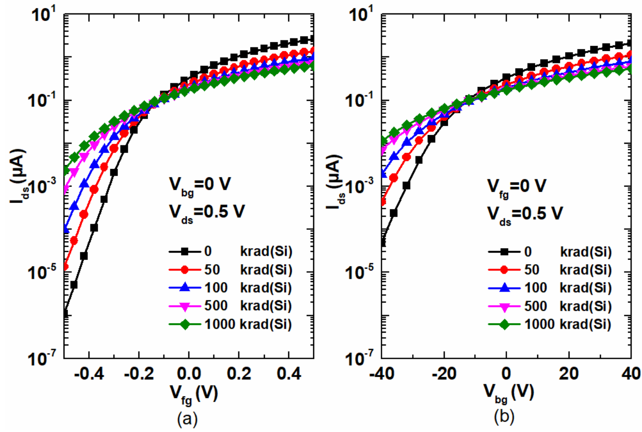

FIGURE 9. Numerical simulations of drain current (I_{ds}) as a function of front gate voltage (V_{fg}) when $V_{ds} = 0.3$ V, $V_{bg} = 0$ V, for a TMDSOI FET ($t_{si} = 0.65$ nm, $t_{oxf} = 2$nm, $t_{oxb} = 90$nm, $W_g = 3$ μm, $L_g = 2.3$ μm), for different values of total dose.

caused by the positive trapped charge in the back gate oxide helps to attract more electron to form inversion layer. In contrast, the saturation current decreases with the increase of TID level, for the reason that mobility degradation becomes to play a dominant role in the irradiated drain current at a larger front gate voltage, which is verified in Fig. 10.

The transconductance is often used to estimate the current amplification ability, which is defined as the variation in the drain current with a small change in the gate voltage [20]. As shown in Fig. 12, transconductance of the TMDOI FET decreases significantly with the increase of total dose level. This can be explained as follows: on one hand, the scattering effect of carrier will be elevated, leading to the reduction of effective carrier mobility; on the other hand, the capture and release of the interface trap will decrease the surface charge.

Fig. 12 (a) plots the threshold voltage shift (ΔV_{TH}) versus TID level, which can be represented as a sum of shifts due to oxide trapped charges (ΔV_{ot}) and interface trapped charges (ΔV_{it}) [21]

$$\Delta V_{TH} = \Delta V_{it} + \Delta V_{ot}. \tag{29}$$

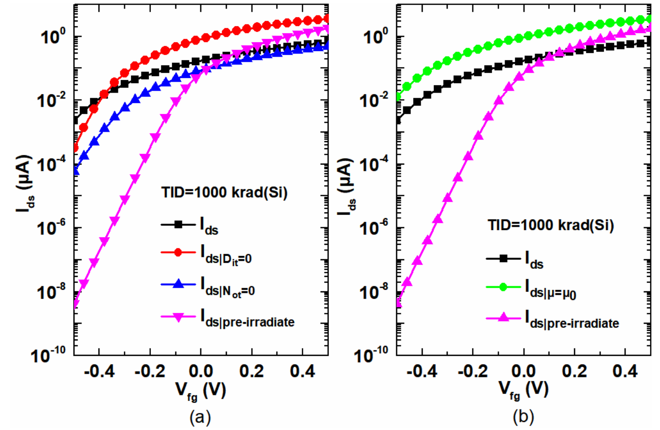

FIGURE 10. (a) Analysis of the contribution of N_{ot} and D_{it} to irradiated drain current for a TMDOI FET, where $I_{ds}|D_{it} = 0$ and $I_{ds}|N_{ot} = 0$ represent for the situations without consideration of N_{ot} and D_{it}, respectively. (b) Analysis of the contribution of mobility degradation to irradiated drain current where $I_{ds}|\mu = \mu_0$ represents for the situation without consideration of mobility degradation.

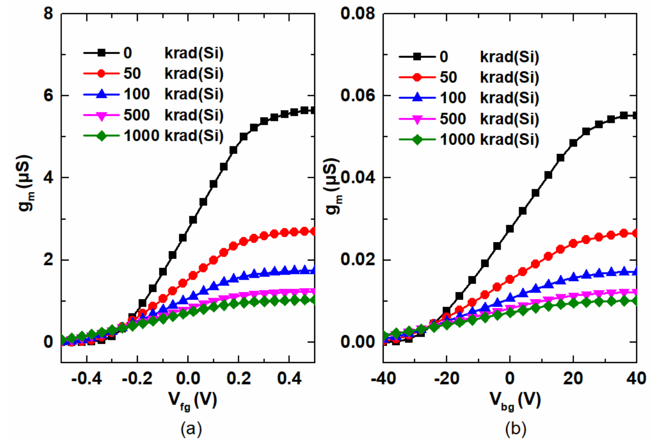

FIGURE 11. Characteristics of the transconductance as a function of front gate voltage, varying total-ionizing dose values.

It is observed that ΔV_{ot} and ΔV_{it} shift in opposite directions, which is the net effect of hole trapping in the SiO_2 layer and electron trapping at the TMD-SiO_2 interface. Previous studies show that ΔV_{it} is proportional to N_{it}, and ΔV_{ot} is proportional to N_{ot} [22], which is obtained as

$$\Delta V_{it} \propto \frac{qN_{it}}{C_{oxf}}, \quad \Delta V_{ot} \propto -\frac{qN_{ot}}{C_{oxf}}. \tag{30}$$

Finally, we can find that the overall effect is a negative shift of threshold voltage mainly due to the comparably thick back gate oxide.

Subthreshold swing (SS) is an important metric to evaluate the conversion rate between on and off states, which can be derived from the magnitude change of gate voltage required for the current values. Fig. 13 (a) plots the subthreshold swing as a function of TID level for TMDOI FET. It can be seen that the SS value increases from around 60 mV/dec to 110 mV/dec after total dose of 1000 krad(Si). It is reported that subthreshold voltage swing is a function of D_{it}, which can

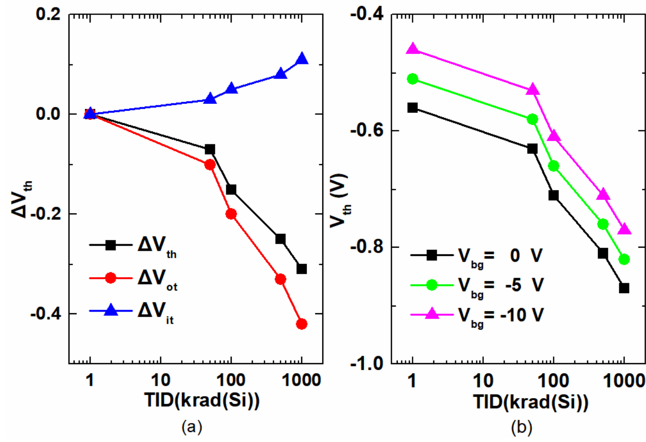

FIGURE 12. Voltage shifts of TMDOI devices as a function of total irradiation dose. The blue line stands for voltage shifts ΔV_{it} due to interfacial trapped charge, voltage shifts due to oxide trapped charge ΔV_{ot} are shown in black, and threshold voltage shifts ΔV_{th} are shown in red.

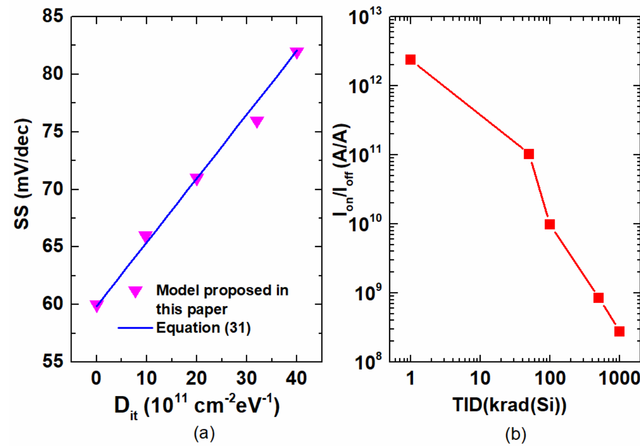

FIGURE 13. (a) Subthreshold swing (*SS*) and (b) I_{ON}/I_{OFF} characteristics as a function of TID level for the TMDOI FET ($W_g = 3\ \mu$m, $L_g = 2.3\ \mu$m, $t_{si} = 0.65$ nm, $t_{oxf} = 2$ nm, $t_{oxb} = 200$ nm).

be expressed as [12]

$$SS \propto v_t \ln(10)\left(1 + \frac{qD_{it}}{C_{oxf}}\right) \tag{31}$$

which is mainly caused by the process of capturing and releasing with the carriers of interface traps, and the effect of oxide traps can be ignored.

Additionally, I_{ON}/I_{OFF} represents the ability of the device to control the channel current. High on-current shows the advantageous capability of output driving, and similarly, low off-current represents a decent ability to turn off the device, which can reduce power consumption. Fig.13 (b) shows the degradation of I_{ON}/I_{OFF} ratio with increasing total dose level, obtained from the transfer characteristic curves of the TMDOI-FET device. It can be found that I_{ON}/I_{OFF} ratio decreases more than three orders of magnitude when total dose is up to 500 krad(Si) which can be explained as the significant increase of the off-state current resulted from the conduction of back gate parasitic transistor, as well as the degradation of mobility caused by the additional interface charge.

To conclude, in order to mitigate the total-ionizing dose effects of TMDOI-FET, some possible solutions can be employed as follows: (1) The back gate oxide thickness should be reduced, so as to minimize the radiation-induced oxide and interface trapped charges. (1) A relatively high energy difference between midgap energy and the Fermi level of the two-dimensional transition metal dischalcogenide should be chosen to decrease the density of interface traps, which can suppress the degradation of effective mobility and subthreshold voltage swing. (3) The back-gate voltage can be applied to decrease the variations of surface potential, and thus mitigate the threshold voltage roll-off and leakage current increase.

V. CONCLUSIONS

In this paper, a surface-potential based drain current model for the bottom-gated TMD FET and TMDOI FET with consideration of total ionizing dose (TID) effects is developed. This model incorporates the impact of oxide trapped charges and interface trapped charges, as well as mobility degradation. The numerical simulation results of a bottom-gated MoS_2 transistor are in good agreement with the experimental data, which validates the proposed approach. To investigate the electrical performance variations of the TMDOI FET, the surface potential and drain current as functions of total dose level are presented and analyzed. Moreover, the impacts of TID effects on transconductance, threshold voltage, subthreshold swing and on/off current ratio are discussed comprehensively.

APPENDIX

To prove the validity of the approximation method in (11) by using Taylor series, we will provide a detailed derivation of the approximation in this section.

After simplification, equation (10) can be written as follows,

$$\frac{u}{v_{th}} = \ln(e^{\frac{Q_s}{q^2 v_{th} N_{DOS}}} - 1). \tag{S1}$$

Assuming $x = \frac{Q_s}{q^2 v_{th} N_{DOS}}$, we can obtain that

$$\frac{u}{v_{th}} = \ln(e^x - 1). \tag{S2}$$

It should be noticed that the Taylor series of e^x can be written as

$$e^x = 1 + x + \frac{x^2}{2!} + \frac{x^3}{3!} + \ldots = \sum_0^{\infty} \frac{x^n}{n!} \tag{S3}$$

Due to $x \approx 0$, we only take the first and second terms of the expansion, which means that $e^x \approx 1 + x$. Based on this, after simplifying equation (S2), we can obtain that

$$\frac{u}{v_{th}} = \ln(e^x - 1) \approx \ln(x + 1 - 1) = \ln(x), \tag{S4}$$

Therefore, it can be given as

$$\varphi_s - V = v_{th} \ln \frac{Q_s}{q^2 v_{th} N_{DOS}}. \quad \text{(S5)}$$

Combining equation (8) into (S5), we can obtain equation (13).

REFERENCES

[1] M.-Y. Li, S.-K. Su, H.-S. P. Wong, and L.-J. Li, "How 2D semiconductors could extend Moore's law," *Nature*, vol. 567, no. 7747, pp. 169–170, Mar. 2019.

[2] Y. Yoon, K. Ganapathi, and S. Salahuddin, "How good can monolayer MoS_2 transistors be?" *Nano Lett.*, vol. 11, no. 9, pp. 3768–3773, Sep. 2011.

[3] G. Fiori, F. Bonaccorso, G. Iannaccone, T. Palacios, D. Neumaier, A. Seabaugh, S. K. Banerjee, and L. Colombo, "Electronics based on two-dimensional materials," *Nature Nanotechnol.*, vol. 9, no. 12, pp. 768–779, Dec. 2014.

[4] A. Splendiani, L. Sun, Y. Zhang, T. Li, J. Kim, C.-Y. Chim, G. Galli, and F. Wang, "Emerging photoluminescence in monolayer MoS_2," *Nano Lett.*, vol. 10, no. 4, pp. 1271–1275, Mar. 2010.

[5] D. M. Fleetwood, "Evolution of total ionizing dose effects in MOS devices with Moore's law scaling," *IEEE Trans. Nucl. Sci.*, vol. 65, no. 8, pp. 1465–1481, Aug. 2018.

[6] E. Simoen, M. Gaillardin, P. Paillet, R. A. Reed, R. D. Schrimpf, M. L. Alles, F. El-Mamouni, D. M. Fleetwood, A. Griffoni, and C. Claeys, "Radiation effects in advanced multiple gate and silicon-on-insulator transistors," *IEEE Trans. Nucl. Sci.*, vol. 60, no. 3, pp. 1970–1991, Jun. 2013.

[7] V. Ferlet-Cavrois, L. W. Massengill, and P. Gouker, "Single event transients in digital CMOS-A review," *IEEE Trans. Nucl. Sci.*, vol. 60, no. 3, pp. 1767–1790, Apr. 2013.

[8] C. X. Zhang, A. K. M. Newaz, B. Wang, E. X. Zhang, G. X. Duan, D. M. Fleetwood, M. L. Alles, R. D. Schrimpf, K. I. Bolotin, and S. T. Pantelides, "Electrical stress and total ionizing dose effects on MoS_2 transistors," *IEEE Trans. Nucl. Sci.*, vol. 61, no. 6, pp. 2862–2867, Dec. 2014.

[9] T.-Y. Kim, K. Cho, W. Park, J. Park, Y. Song, S. Hong, W.-K. Hong, and T. Lee, "Irradiation effects of high-energy proton beams on MoS_2 field effect transistors," *ACS Nano.*, vol. 8, no. 3, pp. 2774–2781, Feb. 2014.

[10] G. I. Zebrev, V. V. Orlov, A. S. Bakerenkov, and V. A. Felitsyn, "Compact modeling of MOSFET $I---V$ characteristics and simulation of dose-dependent drain currents," *IEEE Trans. Nucl. Sci.*, vol. 64, no. 8, pp. 2212–2218, Aug. 2017.

[11] I. S. Esqueda, H. J. Barnaby, and M. P. King, "Compact modeling of total ionizing dose and aging effects in MOS technologies," *IEEE Trans. Nucl. Sci.*, vol. 62, no. 4, pp. 1501–1515, Aug. 2015.

[12] F. Jazaeri, C.-M. Zhang, A. Pezzotta, and C. Enz, "Charge-based modeling of radiation damage in symmetric double-gate MOSFETs," *IEEE J. Electron Devices Soc.*, vol. 6, pp. 85–94, Nov. 2018.

[13] W. Cao, J. Kang, W. Liu, and K. Banerjee, "A compact current-voltage model for 2D semiconductor based field-effect transistors considering interface traps, mobility degradation, and inefficient doping effect," *IEEE Trans. Electron Devices*, vol. 61, no. 12, pp. 4282–4290, Dec. 2014.

[14] M. Hao, H. Hu, B. Wang, C. Liao, H. Kang, and H. Su, "Study on the influence of γ-ray total dose radiation effect on the electrical properties of the uniaxial strained Si nanometer NMOSFET," *Solid-State Electron.*, vol. 133, pp. 45–52, Jul. 2017.

[15] K. F. Galloway, M. Gaitan, and T. J. Russell, "A simple model for separating interface and oxide charge effects in MOS device characteristics," *IEEE Trans. Nucl. Sci.*, vol. NS-31, no. 6, pp. 1497–1501, Dec. 1984.

[16] S. Datta, *Quantum Transport: Atom to Transistor*. Cambridge, U.K.: Cambridge Univ. Press, 2005.

[17] N. Ma and D. Jena, "Carrier statistics and quantum capacitance effects on mobility extraction in two-dimensional crystal semiconductor field-effect transistors," *2D Mater.*, vol. 2, no. 1, Jan. 2015, Art. no. 015003.

[18] C. Yadav, P. Rastogi, T. Zimmer, and Y. S. Chauhan, "Charge-based modeling of transition metal dichalcogenide transistors including ambipolar, trapping, and negative capacitance effects," *IEEE Trans. Electron Devices*, vol. 65, no. 10, pp. 4202–4208, Oct. 2018.

[19] C. Yadav, A. Agarwal, and Y. S. Chauhan, "Compact modeling of transition metal dichalcogenide based thin body transistors and circuit validation," *IEEE Trans. Electron Devices.*, vol. 64, no. 3, pp. 1261–1268, Mar. 2017.

[20] I. J. Umoh, T. J. Kazmierski, and B. M. Al-Hashimi, "A dual-gate graphene FET model for circuit simulation—SPICE implementation," *IEEE Trans. Nanotechnol.*, vol. 12, no. 3, pp. 427–435, May 2013.

[21] J. J. McMorrow, C. D. Cress, H. N. Arnold, V. K. Sangwan, D. Jariwala, S. W. Schmucker, T. J. Marks, and M. C. Hersam, "Vacuum ultraviolet radiation effects on two-dimensional MoS_2 field-effect transistors," *Appl. Phys. Lett.*, vol. 110, no. 7, Feb. 2017, Art. no. 073102.

[22] P. J. McWhorter and P. S. Winokur, "Simple technique for separating the effects of interface traps and trapped-oxide charge in metal-oxide-semiconductor transistors," *Appl. Phys. Lett.*, vol. 48, no. 2, pp. 133–135, Jan. 1986.

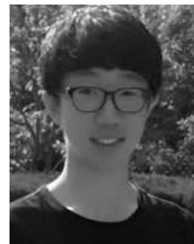

SHUYUN ZHENG was born in Liaoning Province, China, in 1998. He is currently pursuing the undergraduate degree with the Physics and Micro Electronic College, Hunan University, in 2016. He joined as an Assistant Professor Chen's Research Group, in 2017. His research interest includes total-ionizing dose effects on the TMD FETs and compact modeling of SOI FET.

YUN ZENG was born in Hunan Province, China, in 1956. He received the M.S. degree in semiconductor physics and devices from Hunan University, Changsha, China, in 1988. Since 1998, he has been a Full Professor with Hunan University, where he was an Associate Professor, from 1993 to 1998. He has authored more than 180 papers included on the Science Citation Index or the Engineering Index, in national and international journals, and in conference proceedings. He is currently involved in the research and application of electronic devices and relevant teaching. He is a member of the Information and Electronic Teaching Committee of the Chinese Education Ministry, a member of the Technology and Process Committee of the Chinese Computer Federation, and a member of the BES International Collaboration.

ZHUOJUN CHEN received the Ph.D. degree in microelectronics and solid-state circuits with emphasis in radiation-hardened integrated circuit design from Shanghai Institute of Microsystem and Information Technology, Chinese Academy of Sciences, in 2017. After graduation, he is an Assistant Professor with Hunan University. His current research interests include radiation effects of emerging FETs, rad-hard low-power IC, and on-chip ESD protection.